Numerical model for prediction of the Doppler measurement accuracy in the atmospheric boundary layer

A.P. Shelekhov, E.A. Shelekhova, D.A. Belikov, and A.V. Starchenko

V.E. Zuev Institute of Atmospheric Optics, Siberian Branch of the Russian Academy of Sciences, Tomsk

Received January 18, 2008

The paper describes a prognostic model of the Doppler measurement accuracy based on equations for estimating the mean radial wind velocity and the one-dimensional model of the homogeneous atmospheric boundary layer. This model makes possible the numerical prediction of the radial wind velocity, its measurement error, as well as potential temperature, kinetic energy, and the turbulence dissipation rate for the meteorological situation, when the atmospheric stratification varies significantly during daytime. It is shown that the measurement error of mean radial wind velocity can vary widely depending on the day time. During day-time with increasing the turbulence intensity the measurement error grows, and in the evening and at night, when the turbulent boundary layer begins to collapse, the measurement accuracy increases first on the ground surface and then all over the height.

Introduction

At present, the prediction of the Doppler measurement accuracy is performed with the use of simplified atmospheric models based on the empirical dependences for vertical profiles of meteorological parameters.[1] In reality the meteorological situation during daytime significantly varies, that leads to a great divergence between the real atmospheric condition and the data obtained from models of such type. This strongly affects the accuracy of the Doppler measurement prediction.

In this paper, to increase the validity of numerical prediction, the equations for estimating the mean radial wind velocity are closed by equations of the prognostic meteorological model for the atmospheric boundary layer, which take into account diurnal variations of meteorological parameters and the turbulent structure of the atmospheric boundary layer.

Equations for estimating the mean radial wind velocity are written with accounting for the influence of Gaussian and non-Gaussian fluctuations of the Doppler frequency, as well as the nonstationary character of pulse laser radiation scattering by atmospheric particles.

These equations have shown that the Doppler measurements can be interpreted as measurements of mean radial wind velocity only approximately. The measurement error depends on the behavior of profiles of kinetic energy and the rate of dissipation of the turbulence energy, and its magnitude shows to what extent the interpretation of the Doppler sensing data is correct as the mean radial wind velocity.

The one-dimensional prognostic model of the atmospheric boundary layer, used by us, includes nonstationary equations for the horizontal wind component, potential temperature, and humidity. For modeling the turbulent structure of the planetary boundary layer, the "e–l" model of turbulence is used, corresponding to the level 2.5 by the Mellor–Yamada classification.[2–4] For the model initialization, the observation data of vertical structure of the planetary boundary layer, daily variations of geostrophic wind, and the ground temperature are used.

The output parameters are the profiles of basic meteorological characteristics: profiles of the wind velocity and direction, as well as of temperature, pressure, humidity, kinetic energy, and the rate of dissipation of the turbulence energy.

The calculated meteorological characteristics make possible the numerical prediction of the behavior of estimation of the mean radial wind velocity, i.e., the forecast of the behavior of such parameters as the mean radial wind velocity and its measurement error. Hence, the proposed model of the Doppler measurement accuracy, based on the above equations, enables us to interpret correctly the data of lidar sensing in situations, when the meteorological characteristics vary considerably during daytime.

1. Equations for estimation of the radial wind velocity

In the case of the method of autocorrelation function,[1,5,6] the expression for estimation of the Doppler frequency shift has the form:

$$\hat{f}_{\mathrm{d}} = \frac{1}{T_s}\arg\hat{\mathbf{K}}(T_s)\,, \qquad (1)$$

where $\hat{\mathbf{K}}(T_s) = \frac{1}{M}\sum_{q=1}^{M} j^{*}(qT_s)\,j(qT_s + T_s)$ is the estimate of the autocorrelation function, $j(t)$ is the Doppler

0235-6880/08/09 709-06 $02.00

lidar signal, T_s is the interval of discreteness, M is the number of discrete intervals.

The evaluation of the Doppler frequency shift can be written as a sum of a regular part and two fluctuation parts[1]:

$$\hat{f}_{\rm d}(t,z)=f(t,z)+f'_{\rm ng}(t,z)+f'_{\rm g}(t,z), \qquad (2)$$

where

$$f(t,z)=2ku_{\rm r}(t,z)=2k\left[U(t,z)\mathbf{i}_1+V(t,z)\mathbf{i}_2\right]\mathbf{n} \qquad (3)$$

is the regular part of the estimation of the Doppler frequency shift.

$$f'_{\rm ng}(t,z)=\frac{2k}{M}\sum_{q=1}^{M}\int\left|p\left(qT_s-2\frac{|\bar{z}-z_1|}{c},\mathbf{r}_1\right)\right|^2 u'_{\rm r}(t,\mathbf{r}_1){\rm d}\mathbf{r}_1 \qquad (4)$$

is the non-Gaussian part of fluctuations in evaluation of the Doppler frequency shift.

$$f'_{\rm g}(t,z)=\frac{1}{T_s}\frac{\mathbf{K}_{\rm r}(T_s)\Delta\hat{\mathbf{K}}_{\rm i}(T_s)-\mathbf{K}_{\rm i}(T_s)\Delta\hat{\mathbf{K}}_{\rm r}(T_s)}{\left|\mathbf{K}(T_s)\right|^2} \qquad (5)$$

is the Gaussian part of the fluctuations. In Eqs. (2)–(5) $u_{\rm r}(t,z)$ is the mean radial wind velocity, $u'_{\rm r}(t,z)$ are fluctuations of radial wind velocity, $U(t, z)$ and $V(t, z)$ are components of the mean wind velocity along the axes $\mathbf{i}_1$ and $\mathbf{i}_2$; $\mathbf{n}$ is the sensing direction, $\bar{z}$ is the sensing range, $\Delta\hat{\mathbf{K}}(T_s)=\hat{\mathbf{K}}(T_s)-\mathbf{K}(T_s)$; $\mathbf{K}_{\rm r}(T_s)$ and $\Delta\hat{\mathbf{K}}_{\rm r}(T_s)$ are the real parts, $\mathbf{K}_{\rm i}(T_s)$ and $\Delta\hat{\mathbf{K}}_{\rm i}(T_s)$ are the imaginary parts of $\mathbf{K}(T_s)$ and $\Delta\hat{\mathbf{K}}(T_s)$; $\mathbf{K}(T_s)=\left\langle\hat{\mathbf{K}}(T_s)\right\rangle_{\mathbf{r}_m,N_p}$ is the partly averaged autocorrelation function with respect to random position of particles $\mathbf{r}_m$, the number of particles in the scattering volume N_p.[1]

As is evident from the foregoing account, the presentation for estimating the Doppler frequency shift is written with accounting for the influence of Gaussian and non-Gaussian fluctuations of the Doppler frequency, as well as of nonstationary character of scattering the pulse laser radiation by atmospheric particles.[1]

The diagram of lidar directivity $p(t)$ determines the form of the sounding volume, which at the pulse sounding has the form[1,5]

$$p(t,\mathbf{r})\sim\exp(-t^2/\tau_0^2)\delta(\mathbf{r}_\perp),$$

where $2\tau_0$ is the pulse length, $\mathbf{r}_\perp$ is the transverse component of the vector r to the direction $\mathbf{n}$; $\delta(\mathbf{r}_\perp)$ is the Dirac delta-function.

2. The measurement error of the radial wind velocity

It follows from Eqs. (1)–(5) that the expression for estimation of the radial wind velocity may be written in the form:

$$\hat{u}_{\rm r}(t,z)=\frac{1}{2k}\hat{f}_{\rm d}=u_{\rm r}(t,z)+\frac{1}{2k}\left[f'_{\rm ng}(t,z)+f'_{\rm g}(t,z)\right]. \qquad (6)$$

It is seen that the estimate of the radial wind velocity coincides with the radial wind velocity $\hat{u}_r(t,z)=u_r(t,z)$ if the Gaussian and non-Gaussian parts of fluctuations are zero. This means that only at $f'_{\rm ng}(t,z)=f'_{\rm g}(t,z)=0$ the lidar sensing data may be interpreted accurately as measurements of mean radial wind velocity. If $f'_{\rm ng}(t,z)\neq0$ and $f'_{\rm g}(t,z)\neq0$, then the interpretation of lidar sensing data is approximate, i.e.,

$$\hat{u}_{\rm r}(t,z)=u_{\rm r}(t,z)+\Delta\hat{u}_{\rm r}(t,z), \qquad (7)$$

where

$$\Delta\hat{u}_{\rm r}(t,z)=\hat{u}_{\rm r}(t,z)-u_{\rm r}(t,z)=\frac{1}{2k}\left[f'_{\rm ng}(t,z)+f'_{\rm g}(t,z)\right]$$

is the measurement error of the radial wind velocity. Thus, the Gaussian and non-Gaussian parts of Doppler frequency shift fluctuations are the reason for the measurement error of the radial wind velocity.

The measurement error of the radial wind velocity is characterized by the variance value

$$\sigma^2_{u_{\rm r}}(t,z)=\left\langle\left[\hat{u}_{\rm r}(t,z)-u_{\rm r}(t,z)\right]^2\right\rangle. \qquad (8)$$

Calculations of the variance of measurement error of the radial wind velocity by Eq. (1)–(8) result in the following expression

$$\sigma^2_{u_{\rm r}}(t,z)=\frac{1}{M^2}\sum_{q_1,q_2=1}^{M}\int\left|p\left(q_1T_s-2\frac{|\bar{z}-z_1|}{c},\mathbf{r}_1\right)\right|^2\times$$

$$\times\left|p\left(q_2T_s-2\frac{|\bar{z}-z_2|}{c},\mathbf{r}_2\right)\right|^2 R_{u'_{\rm r}}(t,\mathbf{r}_1,\mathbf{r}_2){\rm d}\mathbf{r}_1{\rm d}\mathbf{r}_2+\frac{1}{8k^2MT_s^2}\times$$

$$\times\left\{T_s\sqrt{\pi\left(\Delta\omega^2_{\tau_0}+\left\langle\Delta\omega'^2_{\rm d,ng}\right\rangle\right)}+\frac{N}{S}T_s^2\left(\Delta\omega^2_{\tau_0}+\left\langle\Delta\omega'^2_{\rm d,ng}\right\rangle\right)+\frac{N^2}{S^2}\right\}, \qquad (9)$$

where

$$\left\langle\Delta\omega'^2_{\rm d,ng}\right\rangle=\frac{1}{2M}\sum_{q=1}^{M}\int\left|p\left(qT_s-2\frac{|\bar{z}-z_1|}{c},\mathbf{r}_1\right)\right|^2\times$$

$$\times\left|p\left(qT_s-2\frac{|\bar{z}-z_2|}{c},\mathbf{r}_2\right)\right|^2 D_{\omega'_{\rm d}}(\mathbf{r}_1,\mathbf{r}_2){\rm d}\mathbf{r}_1{\rm d}\mathbf{r}_2 \qquad (10)$$

is the turbulent spectral width, $\Delta\omega^2_{\tau_0}=1/2\tau_0^2$; S/N is the signal-to-noise ratio,

$$R_{u'_{\rm d}}(t,\mathbf{r}_1,\mathbf{r}_2)=\sum_{k,l}\left\langle u'_k(t,\mathbf{r}_1)u'_l(t,\mathbf{r}_2)\right\rangle n_k n_l;$$

are coordinates of vector **n;**

$$D_{\omega_d'}(\mathbf{r}_1,\mathbf{r}_2)=4k^2\sum_{k,l}\left\langle\left(u_k'(\mathbf{r}_1)-u_k'(\mathbf{r}_2)\right)\left(u_l'(\mathbf{r}_1)-u_l'(\mathbf{r}_2)\right)\right\rangle n_k n_l.$$

3. Measurement error of the radial wind velocity in case of "2/3 law"

In case of the "2/3 law"[4] in the behavior of the measurement error of the radial wind velocity three cases should be considered, depending on the condition of the turbulent atmosphere and dimensions of the scattering volume. The first case is observed at $\varepsilon(t,z)d_{v,\mathrm{eff}}\ll e(t,z)^{3/2}$, where $e(t,z)$ $e(t,\ z)$ is the kinetic energy $\varepsilon(t,z)$ is the velocity of turbulence dissipation energy; $2d_{v,\mathrm{eff}}=2d_v+MT_sc/2$ is the length of the scattering volume, $2d_v=c\tau_0$.[1,5] For the Gaussian approximation of the form of the scattering volume, the expression for the error variance is of the form

$$\sigma_{u_r}^2(t,z)=e(t,z)-0.401C^2\left(\varepsilon(t,z)d_{v,\mathrm{eff}}\right)^{2/3}+$$

$$+\frac{1}{8k^2MT_s^2}\left\{2kT_s\sqrt{\pi\left(\Delta\omega_{\tau_0}^2+0.401C^2(\varepsilon(t,z)d_v)^{2/3}\right)}+\right.$$

$$\left.+16k^2T_s^2\frac{N}{S}\left[\Delta\omega_{\tau_0}^2+0.401C^2\left(\varepsilon(t,z)d_v\right)^{2/3}\right]+\frac{N^2}{S^2}\right\}. \quad (11)$$

The second case is observed at $\varepsilon(t,\ z)d_{v,\mathrm{ef}}\gg e(t,\ z)\gg\varepsilon(t,\ z)d$. For the error variance we have the following expression

$$\sigma_{u_r}^2=\frac{1}{8k^2MT_s^2}\left\{2kT_s\sqrt{\pi\left(\Delta\omega_{\tau_0}^2+0.401C^2\left(\varepsilon(t,z)d_v\right)^{2/3}\right)}+\right.$$

$$\left.+16k^2T_s^2\frac{N}{S}\left[\Delta\omega_{\tau_0}^2+0.401C^2\left(\varepsilon(t,z)d_v\right)^{2/3}\right]+\frac{N^2}{S^2}\right\}. \quad (12)$$

When $\varepsilon(t,z)d_v\gg e(t,z)^{3/2}$, i.e., in the third case, the expression for the error variance can be written in the form

$$\sigma_{u_r}^2=\frac{1}{8k^2MT_s^2}\left\{2kT_s\sqrt{\pi\left(\Delta\omega_{\tau_0}^2+e(t,z)\right)}+\right.$$

$$\left.+16k^2T_s^2\frac{N}{S}\left[\Delta\omega_{\tau_0}^2+e(t,z)\right]+\frac{N^2}{S^2}\right\}. \quad (13)$$

In Eqs. (11)–(13) $C^2=1.77\pm0.08$. It follows from Eqs. (11)–(13) that the behavior of variance of the measurement error $\sigma_{u_r}^2$ is determined by the behavior of kinetic energy $e(t,\ z)$ and by the velocity of the turbulence dissipation energy $\varepsilon(t,\ z)$. The calculation of $e(t,\ z)$ and $\varepsilon(t,\ z)$ is performed with the use of the model of the planetary boundary layer and "e–l" model of the atmospheric turbulence.

4. Model of the planetary boundary layer

Now we present three components of the wind velocity field, potential temperature, and humidity as a sum of mean and fluctuation components:

$$u(t,z)=U(t,z)+u'(t,z);$$

$$v(t,z)=V(t,z)+v'(t,z);$$

$$w(t,z)=W(t,z)+w'(t,z),\ \ W(t,z)=0; \quad (14)$$

$$\theta(t,z)=\Theta(t,z)+\theta'(t,z);$$

$$q(t,z)=Q(t,z)+q'(t,z).$$

In case of one-dimensional model of the homogeneous atmospheric boundary layer, the equations for components of mean horizontal wind velocity $U(t,\ z)$ and $V(t,\ z)$, mean temperature $\theta(t,\ z)$ and mean humidity $Q(t,\ z)$ are of the form[2,3]:

$$\frac{\partial U}{\partial t}=-\langle u'w'\rangle+f\left(V-V_g\right),\ \ \frac{\partial V}{\partial t}=-\langle v'w'\rangle+f\left(U-U_g\right), \quad (15)$$

$$\frac{\partial\Theta}{\partial t}=-\langle\theta'w'\rangle,\ \ \frac{\partial Q}{\partial t}=-\langle q'w'\rangle, \quad (16)$$

where

$$U_g=-\frac{1}{\rho f}\frac{\partial P}{\partial y},\ \ V_g=\frac{1}{\rho f}\frac{\partial P}{\partial x}$$

are components of the geostrophic wind, t is the time, z is the vertical coordinate; ρ is the density, P is the pressure, $f=2\Omega\sin\psi$ is the Coriolis parameter, ψ is the geographic latitude, Ω is the angular velocity of the Earth rotation. For closing equations (14)–(16) the "e–l" model of atmospheric turbulence[2,3] is used.

5. "e–l" model of atmospheric turbulence

The used "e–l" model of atmospheric turbulence includes the transfer equations for kinetic energy $e=\left(\frac{1}{2}\langle u'^2\rangle+\langle v'^2\rangle+\langle w'^2\rangle\right)$, the scale of turbulent fluctuations l [Refs. 2, 3]:

$$\frac{\partial e}{\partial t}=-\langle u'w'\rangle\frac{\partial U}{\partial z}-\langle v'w'\rangle\frac{\partial V}{\partial z}+$$

$$+\frac{g}{\Theta}\langle\theta'w'\rangle+\frac{\partial}{\partial z}\left(\sigma_e\sqrt{el}\frac{\partial e}{\partial z}\right)-\frac{C_De^{3/2}}{l}, \quad (17)$$

$$\frac{\partial l}{\partial t} = C_{L1}\left(-\langle u'w'\rangle\frac{\partial U}{\partial z} - \langle v'w'\rangle\frac{\partial V}{\partial z} + \frac{g}{\Theta}\langle\theta'w'\rangle\right)\frac{l}{e} +$$

$$+\frac{\partial}{\partial z}\left(\sigma_e\sqrt{e}l\frac{\partial l}{\partial z}\right) + C_{L2}\sqrt{e}\left[1-\left(\frac{l}{\kappa z}\right)^2\right]; \qquad (18)$$

$$\varepsilon = \frac{C_D e^{3/2}}{l}, \quad \langle u'w'\rangle = -F_m\sqrt{e}l\frac{\partial U}{\partial z},$$

$$\langle v'w'\rangle = -F_m\sqrt{e}l\frac{\partial V}{\partial z}, \quad \langle\theta'w'\rangle = -F_h\sqrt{e}l\frac{\partial\Theta}{\partial z}, \qquad (19)$$

where $\sigma = 0.54$, $C_{L1} = -0.12$, $C_{L2} = 0.2$, $C_D = 0.19$, $\kappa = 0.4$, F_m and F_h are the functions of local turbulent characteristics,[2,3] "$e-l$" model of atmospheric turbulence (17)–(19), corresponds to the level 2.5 according to the Mellor–Yamada classification.[4]

The boundary conditions for Eqs. (15)–(19) are formulated as follows[2,3]:

at $z = z_1 >> z_0$

$$U = \frac{v_*}{\kappa}f_u(\zeta_1)\cos\beta; \quad V = \frac{v_*}{\kappa}f_u(\zeta_1)\sin\beta; \qquad (20)$$

$$\Theta = \Theta_1^{obs}(t); \quad Q = Q_1^{obs}(t); \quad e = v_*^2 f_k(\zeta_1); \quad l = \kappa z_1 f_l(\zeta_1); \qquad (21)$$

at $z = H$

$$\frac{\partial U}{\partial z} = \frac{\partial V}{\partial z} = \frac{\partial k}{\partial z} = \frac{\partial l}{\partial z} = \frac{\partial Q}{\partial z} = 0, \quad \frac{\partial\Theta}{\partial z} = \gamma, \qquad (22)$$

where z_0, z_l, H are the roughness parameter, the height of position of the first calculated level, and the height of the calculation range, respectively; f_u, f_k, f_l are the empirical functions,[2,3] $\zeta_l = z/L$, β is the angle between the vector of the surface wind velocity and the axis Ox, $\theta_l^{obs}(t)$, $Q_1^{obs}(t)$ are functions, determining the dependence on temperature and air humidity at a height of 2 m; L is the Monin–Obukhov scale.

Initial conditions for Eqs. (15) and (16) are set in accordance with the results of processing of measurements of vertical structure of the atmospheric boundary layer. For equations (17)–(19), intended for determination of turbulent characteristics, the initial data are generated by the preliminary calculations, using the presented model with the use of the fixed initial distributions for dynamic and thermodynamic parameters of the atmospheric boundary layer.

6. Results of numerical simulation

In this paper, the prediction of Doppler measurement accuracy was made for the synoptic meteorological situation, which was observed in Tomsk on May 27, 2004. Measurements of the State Hydrometeorological Center at meteorological stations of Kolpashevo, Novosibirsk, Kemerovo, and Tomsk were used to initialize the model.

Figure 1 shows the results of the calculated wind velocity and direction, potential temperature, kinetic energy, and the dissipation energy rate. The numerical forecast shows that the meteorological situation that day varied greatly. A stable stratification was observed at the beginning of daytime, and as the solar activity increased and the Earth's surface was heated, the stratification first became neutral and then unstable. After the sunset and the Earth surface cooling the atmospheric condition varied from unstable stratification to stable one.

The solar activity, surface heating, and other factors lead to appearance of the turbulent boundary layer of different intensities in different times of day. Thus, at nighttime the intensity of atmospheric turbulence is low. After the sunrise and at the surface heating, the noticeable turbulent boundary layer begins to form. By 8:00 pm the turbulent boundary layer is formed completely, and its height reaches 2000 m. After 8:00 pm the solar activity begins to decrease, the ground surface cools, and the collapse of the turbulent boundary layer begins first at the Earth's surface and then through the whole height. As a result, the kinetic energy and the energy of turbulence dissipation at night-time decrease and at daytime increase significantly.

Figure 2 shows the results of numerical forecast of the profile of the radial wind velocity, as well as the profile of its measurement error for the following parameters of the Doppler lidar: $\lambda = 2$ μm; $M = 16$; $T = 0.02$ μs, $\tau_0 = 0.12$ μs. When calculating the profile of radial wind velocity, it was assumed that the sensing direction vector **n** was in the plane $\{i_1, i_3\}$, and the sensing cone angle was equal to 45°.

At nighttime, when low turbulence intensity is observed, the measurement error does not exceed the value of radial wind velocity. After the sunrise, heating the surface and forming the turbulent boundary layer, the measurement accuracy begins to fall first at small heights. By the time of a complete formation of the turbulent boundary layer, which extends to the heights of 2000 m, the measurement accuracy decreases throughout the heights and its magnitude is compared with that of radial wind velocity. By the nighttime, as the turbulent boundary layer is destructed, the measurement accuracy of mean radial wind velocity begins to increase first at the Earth surface and then throughout the height.

It follows from Fig. 1, that when the situation during daytime varies, the meteorological characteristics differ considerably from the simplified atmospheric models based on the empirical dependences for vertical profiles of these parameters. For instance, the wind velocity profile for the daytime, corresponding to 2:00 am, 2:00 pm, and 10:00 pm differs greatly from the profile of the same parameter for simplified models of the atmosphere. Only at 8:00 pm it can be considered to be close to the known dependence: the logarithmic profile.[4]

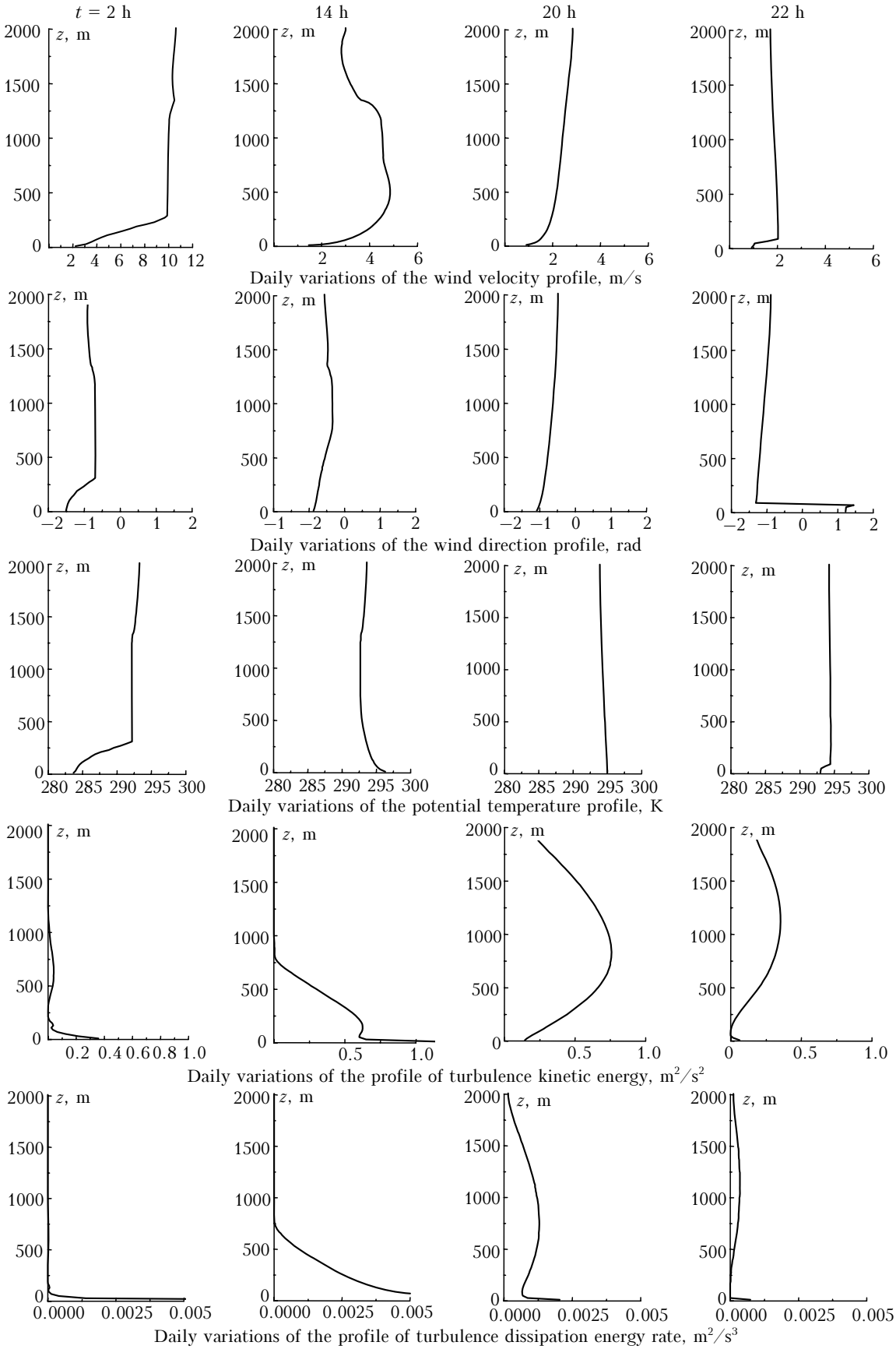
t = 2 h
14 h
20 h
22 h
z, m
Daily variations of the wind velocity profile, m/s
Daily variations of the wind direction profile, rad
Daily variations of the potential temperature profile, K
Daily variations of the profile of turbulence kinetic energy, m²/s²
Daily variations of the profile of turbulence dissipation energy rate, m²/s³

Fig. 1.

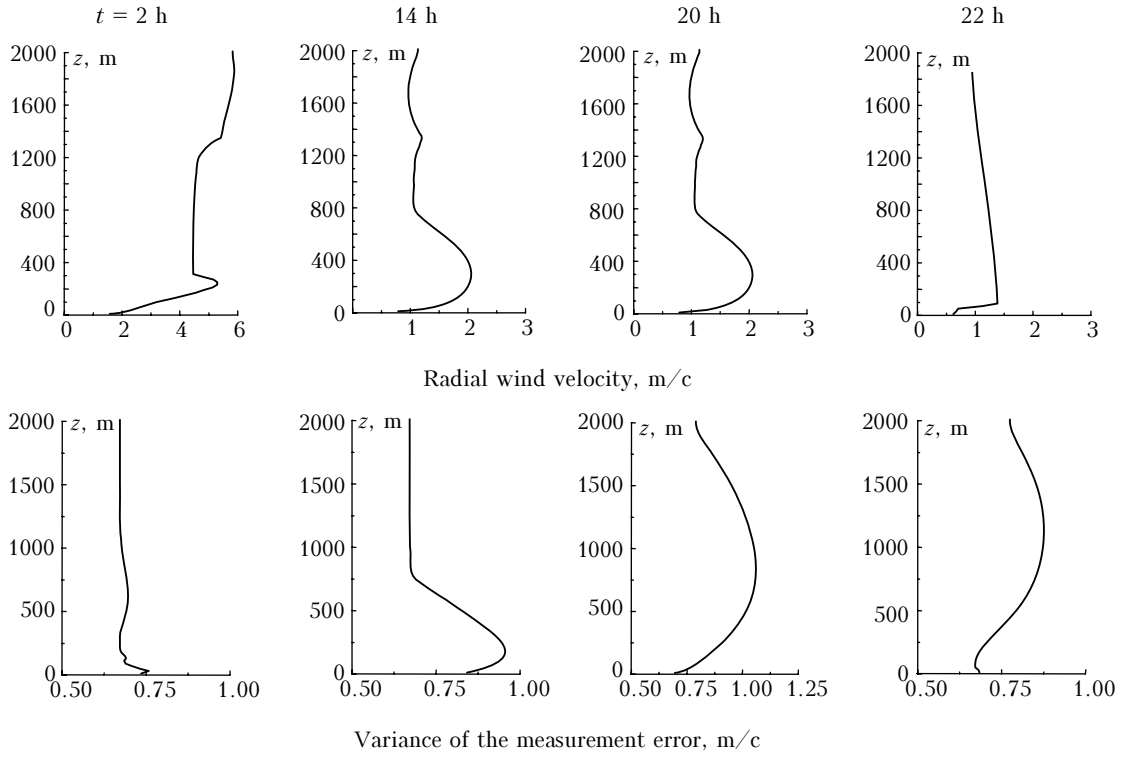

Fig. 2.

The similar situation is observed when analyzing the profiles of kinetic energy and the dissipation energy rate. It is evident that only at 8:00 pm the behavior of these profiles corresponds to empirical dependences for vertical profiles of these parameters.

Thus, for the considered meteorological situation, the simplified atmospheric models can be used only for a short interval of daytime. At the rest of time it is necessary to use more complicated models for predicting the meteorological situation in the atmosphere. This means that the validity of prediction of the Doppler measurement accuracy will be obtained not at the sacrifice of simplified atmospheric models, but on the basis of more complicated prediction equations of the atmosphere, which take into account daily variations of meteorological parameters and turbulent structure of the atmospheric boundary layer.

6. Conclusions

In this paper, the prognostic model of the Doppler measurement accuracy is proposed, based on equations for estimating mean radial wind velocity, and one-dimensional model of the homogeneous atmospheric boundary layer. This model makes it possible to perform the numerical prediction of the radial wind velocity, its measurement error, as well as the potential temperature, kinetic energy, the turbulence dissipation rate for meteorological situation, when the atmospheric stratification varies considerably during 24 hr period. It is shown that the increase of turbulence intensity at daytime yields a marked increase of the measurement error of mean radial wind velocity, as compared to the nighttime. In the evening and at nighttime, when the boundary turbulent layer begins to destruct, the measurement accuracy increases first at the ground surface and then throughout the height of the layer.

References

1. A.P. Shelekhov, in: *Proc. of the 11th Coherent Laser Radar Conf.*, Malvern. UK (2001), pp. 70–73.
2. A.V. Starchenko and D.A. Belikov, Atmos. Oceanic Opt. **16**, No. 7, 608–615 (2003).
3. A.V. Starchenko, in: *Proc. of Int. Conf. ENVIROMIS 2000*, Tomsk (2000), pp. 77–82.
4. R.B. Stull, *An Introduction to Boundary Layer Meteorology* (Kluwer Academic Publishers, Atmos. Sci. Library, Netherlands, 1989), 666 pp.
5. R.G. Frehlich and M.J. Yadlowsky, J. Atmos. and Ocean. Technol. **11**, No. 5, 1217–1230 (1994).
6. B.J. Ray and R.M. Hardesty, IEEE Trans. Geosci. and Remote Sens. **31**, 28–35 (1993).